Fish and Shellfish Immunology 104 (2020) 497–505

Contents lists available at ScienceDirect

Fish and Shellfish Immunology

journal homepage: www.elsevier.com/locate/fsi

Short communication

Identification and characterization of cystatin B from black rockfish, *Sebastes schlegelii,* indicating its potent immunological importance

P.D.S.U. Wickramasinghe[a,b,1], Hyukjae Kwon[a,c,1], Don Anushka Sandaruwan Elvitigala[d,**], Qiang Wan[a,c], Jehee Lee[a,c,*]

[a] Department of Marine Life Sciences & Fish Vaccine Research Center, Jeju National University, Jeju Self-Governing Province, 63243, Republic of Korea
[b] Department of Chemistry, Faculty of Science, University of Colombo, Colombo-03, Sri Lanka
[c] Marine Science Institute, Jeju National University, Jeju Self-Governing Province, 63333, Republic of Korea
[d] Dept. of Basic Science and Social Sciences for Nursing, Faculty of Nursing, University of Colombo, Thalapathpitiya, Nugegoda, 10250, Sri Lanka

A B S T R A C T

Cystatins represent a large superfamily of proteins involved in the competitive reversible inhibition of C1 class cysteine proteases. Plant-derived papain proteases and cysteine cathepsins are the major cysteine proteases that interact with cystatins. The cystatin superfamily can be further classified into three groups: stefins, cystatins, and kininogens. Among these, cystatin B is categorized under stefins. Cystatin B lacks a signal sequence, disulfide bonds, and carbohydrate groups. However, it contains the conserved cystatin family signature, including a single cystatin-like domain, cysteine protease inhibitory signature concealing pentapeptide (QXVXG) consensus sequence, and two conserved neighboring glycine (^{8}GG^{9}) residues at the N-terminal. In the current study, a member of cystatin B was identified from Korean black rockfish (*Sebastes schlegeli*) using a cDNA database and designated as RfCytB. The full-length cDNA of RfCytB was 573 bp long, with a coding region of 294 bp. The 5′-untranslated region (UTR) comprised 55 bp, and the 263-bp-long 3′-UTR included a polyadenylation signal sequence and a poly-A tail. The coding sequence encodes a polypeptide comprising 97 amino acids, with a predicted molecular weight of 11 kDa and theoretical isoelectric point of 6.3. RfCytB shared homology features with similar molecules from other teleost and vertebrate species, and was clustered with Cystatin family 1 in our phylogenetic reconstruction. RfCytB was ubiquitously expressed in all tissue types of healthy animals, with the highest levels of expression observed in gill and spleen. Temporal expression of *RfCytB* displayed significant up-regulation upon infection with *Aeromonas salmonicida*. Recombinantly expressed RfCytB showed a concentration-dependent inhibitory activity towards papain, with a high thermal stability. Transient expression of *RfCytB* in LPS activated murine macrophages, thereby inducing the expression of genes related to pro-inflammatory conditions, such as iNOS and TNF α. These results provide evidence for its protease inhibitory and immunity relevant roles in hosts.

1. Introduction

Proteases represent a widely distributed group of enzymes found in all living organisms, which play an indispensable role by catalyzing the hydrolysis of peptides bonds in proteins at the cellular level. According to the chemical groups involved in the catalytic process, proteases can be categorized into five major groups: serine, cysteine, aspartic, threonine, and metallo proteases [1]. Among them, cysteine proteases have been identified among almost all taxonomic groups of organisms, including prokaryotes such as viruses and bacteria, showing a ubiquitous distribution [2]. Protein processing by restricted cleavage is a crucial characteristic of cysteine proteases, which helps them play a significant role in antigen presentation, photolytic processing of proenzymes and prohormones, fertilization, cell proliferation, differentiation, and apoptosis in living creatures [3,4]. Cytosolic calpains and lysosomal cathepsins have been identified as major groups of cysteine proteases in mammals [1,5], whereas papain is a well-characterized cysteine protease in plants [6]. All the cysteine proteases with a high structural similarity to papain are categorized into a large single group known as papain family [7].

Cystatins represent a large group of evolutionarily related reversible inhibitors of cysteine proteases, which basically interact with papain family proteases, including mammalian cathepsins B, H, and L [8]. Cystatins are known to inhibit the activity of target proteases by indirectly obstructing the catalytic centers, to prevent the docking and cleavage of substrates [9]. Based on the size of polypeptide chain and the presence or absence of the disulfide bonds, cystatin super family has been subdivided into three major families: family 1, known as stefins,

* Corresponding authorrine Molecular Genetics Lab, Department of Marine Life Sciences, Jeju National University, 102 Jejudaehakno, Jeju, 63243, Republic of Korea.
** Corresponding author.
E-mail addresses: anushka@dss.cmb.ac.lk (D.A.S. Elvitigala), jehee@jejunu.ac.kr (J. Lee).
[1] These authors contributed equally to this work.

https://doi.org/10.1016/j.fsi.2020.05.068
Received 1 October 2019; Received in revised form 9 May 2020; Accepted 25 May 2020
Available online 10 June 2020
1050-4648/

Table 1
Oligomers used in the study.

Name	Application	Sequence (5′ →3′)
RfCytB-qL	qPCR of *RfCytB*	GAGGATCACGTTCACCTCCGTGTTTA
RfCytB-qR	qPCR of *RfCytB*	CAATCTCGTCATCGGAGGACTTGGA
RfEF1A-F	qPCR of *RfCytB*	AACCTGACCACTGAGGTGAAGTCTG
RfEF1A-R	qPCR of *RfCytB*	TCCTTGACGGACACGTTCTTGATGTT
RfCytB -CL	Cloning for pMAL-c2x	GAGAGAgaattcATGATGTGTGGAGGGATTGGAGAAGTTAAG
RfCytB –CR	Cloning for pMAL-c2x	GAGAGAaagcttTTAGAAGTACTCAATCTCGTCATCGGAGGA
RfCytB -TL	Cloning for pcDNA3.1/HisC	GAGAGAgaattcgtgatgggaATGATGTGTGGAGGGATTGGAGAAGTTAAG
RfCytB -TR	Cloning for pcDNA3.1/HisC	GAGAGActcgagTTAGAAGTACTCAATCTCGTCATCGGAGGA

family 2, known as cystatins, and family 3, designated as kininogens [10]. Besides these three groups, novel proteases identified as cystatin family members that share substantial sequence similarity with the existing cystatins but lack the cysteine protease inhibitory properties were categorized under a new family, called family 4 [11,12].

Based on the higher inhibitory potential exerted on cysteine proteases, cystatins play several defensive roles and regulatory functions during various cellular events. For instance, recent studies have reported that cystatins induce NO production via stimulation of TNF-α and IL-10 synthesis, a crucial defense strategy evoked in response to pathogen infections [13,14]. Moreover, teleostan cystatin B molecules exhibit *in vitro* antibacterial [15] and antifungal properties, and inhibit apoptosis in the cerebellum [16,17]. These roles were further elaborated in a variety of teleosts, including *Carassius auratus* [18], *Gadus morhua* [19], *Lates calcarifer* [20], *Cyclopterus lumpus* [21], and *Salmo salar* [22], by transcriptome and proteome analysis under different immune stimulated conditions. Although there exist a few molecular level studies on different cystatin family members from higher vertebrate lineages, detailed characterization of their lower vertebrate counterparts has been reported much more abundantly, except for a few species, including *Oplegnathus faciatus* [23] and *Scophthalmus maximus* [15].

As edible marine fish are considered a protein-rich food source for human diet, there has been a recent push for fish farming, to compensate for the increasing demand. However, because of intensive large-scale culturing of fish in restricted areas, different stress factors, especially pathogenic stress, have adversely affected the mariculture yield of fish worldwide, resulting in a considerable economic loss. Against this backdrop, investigations on molecular pathophysiology of mariculturable fish species can be considered as a first step towards developing disease management strategies against the growing threat of pathogenic infections.

In the current study, a homolog of cystatin B was identified from black rockfish (*Sebastes schlegelii*) and molecularly characterized in terms of *in-silico* profiling and expression analysis in selected tissues under healthy and septic conditions, and was functionally characterized using a recombinant protein.

2. Materials and methods

2.1. Sequence identification and in silico analysis

Based on the alignments obtained from the NCBI Genbank sequence database for our previously reported black rockfish cDNA sequence database [24] using Basic Local Alignment Tool (BLAST), a homolog of cystatin B sequence, designated as RfCytB, was identified. The identified sequence was then used to demarcate the putative open reading frame (ORF) and subsequently derive the corresponding amino acid sequence using the DNAsist 2.2 software package. Sequence comparison studies of predicted protein sequence with its homologues were performed using ClustalW2 program (multiple sequence alignment [25]) and Matgat (pairwise sequence alignment [26]) programs. For investigating the evolutionary relationship with its counterpart molecules, phylogenic analysis of RfCytB was carried out using the Neighbor-joining method, with bootstrapping values taken from 1000 replicates, in Molecular evolutionary genetics Analysis (MEGA) software, version 6 [27]. Characteristic signatures of the RfCytB protein sequence were predicted by ExPASy-prosite server (http://prosite.expasy.org) and some of the physicochemical properties were identified using ExPASy ProtParam tool (http://web.expasy.org/protparam).

2.2. Preparations of RfCytB recombinant plasmid constructs

The coding sequence of the RfCytB was PCR-amplified using corresponding oligomers designed with using restriction enzyme sites (RfCytB-F, RfCytB-R) compatible with the pMAL c2X plasmid vector (New England Biolabs, USA) or pCDNA™3.1/HisC (Life Technologies, US; Table 1). The PCR was carried out in a TaKaRa thermal cycler using a 50 μL total volume, containing 5 U of Ex Taq polymerase (TaKaRa, Japan), 5 μL of 10 × Ex Taq buffer, 0.4 mM of dNTPs, 80 ng of template, and 10 pmol of each oligomer. The reaction conditions were: initial incubation at 94 °C for 4 min, followed by 35 cycles of 94 °C for 30 s, 55 °C for 30 s, and 72 °C for 45 s, and a final extension at 72 °C for 3 min. Subsequently, the pMAL-c2X vector and amplified products were digested with respective restriction enzymes and analyzed by gel electrophoresis. Fragments matched with the expected size were excised, purified using the Accuprep gel purification kit (Bioneer Co., Korea), and ligated into pMAL-c2X by overnight incubation with Mighty Mix (TaKaRa) at 4 °C to prepare the pMAL-c2X/*RfCytB* fusion construct. On the following day, the ligated product was transformed into *Escherichia coli* (*E. coli*) DH5α cells. Finally, cloning of the coding region of RfCytB was confirmed by sequencing at Macrogen-Korea.

2.3. Over-expression and purification of recombinant RfCytB

RfCytB recombinant fusion constructs were transformed into *E.coli* BL21 (DE3) competent cells, and the respective putative single colonies bearing the constructs with the deleted and complete coding regions were selected. The selected colonies were separately grown overnight in 500 mL of LB broth medium, supplemented with 100 μg/mL ampicillin at 37 °C with shaking (200 rpm). After the optical density (OD) at 600 nm reached 0.6, isopropyl-β-thiogalactopyranoside (IPTG) was mixed at a final concentration of 0.5 mM, and the final mixture was incubated for 8 h at 20 °C to induce recombinant protein expression. Subsequently, the cells were cooled on ice for 30 min and harvested by centrifugation at 3000 × *g* for 30 min at 4 °C. The obtained pellets were resuspended in column buffer (20 mM Tris-HCl, pH 7.4 and 200 mM NaCl) and stored overnight at −20 °C. On the following day, the cells were thawed under chilled conditions and ruptured by cold sonication in the presence of lysozyme (1 mg/mL). The resultant solution was separated by centrifugation (9000 × *g* for 30 min at 4 °C). The supernatant was defined as a crude extract and the recombinant proteins (complete and deleted products) were purified using pMAL protein fusion and purification technique (New England BioLabsInc, USA). Subsequently, the concentration of the purified fusion protein products was determined using the Bradford method. The rRfCytB-MBP fusion

product was cleaved using Factor Xa, according to the pMAL™ Protein Fusion and Purification kit protocol, with the resultant cleaved protein product mixture (rRfCytB) used for functional assays. The samples collected at different steps of the rRfCytB purification were analyzed using 12% SDS-PAGE under reduced conditions using standard protein size markers (Enzynomics, Korea), confirming sufficient purity along with integrity of the fusion protein and its successful cleavage by factor Xa.

2.4. Papain inhibitory activity assay

Cysteine protease inhibitory activity of rRfCytB was evaluated against crude papain (P3375; Sigma-Aldrich, St, Louis, MO, USA) according to a previously published method with some modifications [27]. Briefly, crude papain was dissolved in potassium phosphate buffer (PPB; pH-7.6) to obtain a final concentration of 1 mg/mL, following which, 10 μL of the solution was mixed with different volumes of rRfCytB to meet 0/1 (negative control), 1/8, 1/4, 1/2, 1, 2, 3, 4, and 5 rRfCytB/papain concentration ratios in a final PPB volume of 120 μL. Subsequently, the mixture was incubated at 25 °C for 15 min and 50 μL of azo casein (0.5%) was added to each mixture before incubation at 37 °C for 20 min, after proper mixing. Thereafter, the reaction was terminated by adding 100 μL of 10% trichloroacetic acid to the final reaction mixtures. Finally, the mixtures were centrifuged and the supernatant was used for OD measurements at 440 nm. One control experiment was carried out using equal amounts of elution buffer (column buffer + 10 mM maltose) instead of the protein. Another control experiment was carried out using MBP treated with factor Xa (MBP/papain concentration ratio = 5) instead of rRfCytB, following the same experimental procedure, to investigate the effect of MBP on the activity in cleaved rRfCytB. The relative inhibitory activity was calculated as: $100 \times [1 - (OD_{440}$ of protein-treated sample/OD_{440} of negative control)]. All the assays were carried out in triplicate and the data are presented as the mean of these replicates. Moreover, the experiment was repeated using 4:1 rRfCytB/papain ratio after heating the rRfCytB protein at 90 °C for 0, 10, 20, 30, 40, 50, and 60 min, to assess the thermal stability of the protein using triplicate assays.

2.5. Construction of expression vector and transfection assay

2.5.1. Construction of expression vector

The full-length CDS of RfCytB (294 bp) was PCR-amplified from gill cDNA using gene-specific primers (Table 1) and then subcloned into pcDNA3.1/HisC (Life Technologies, US). The clone harboring the RfCytB CDS was confirmed by sequencing and termed as pcDNA-RfCytB.

2.5.2. Cell culture and transfection

Murine macrophage cells were grown in Dulbecco Modified Eagle Medium (DMEM- WELGENE-Korea) supplemented with 10% fetal bovine serum (FBS) and maintained at 37 °C in 5% CO_2. The prepared pcDNA-RfCytB recombinant construct was transiently transfected into Murine Macrophage cells using the X-tremeGENE™ 9 DNA Transfection Reagent (Roche, USA), following the manufacturer's instructions. After the transfection, over-expression of RfCytB was confirmed by a qPCR assay conducted on transfected, mock controls (empty pcDNA3.1/HisC) and transfection controls (without vector) by comparing the expression level with the un-transfected control. Murine β-actin gene was used as the internal control (GenBank ID: AAI38615) and the corresponding primer pair (Table 1) for RfCytB was used for the qPCR. The transfected cell lines were treated with LPS at 24 h after the transfection to activate and induce inflammatory conditions in cells, and the expressional modulation of TNFα and iNOS genes was analyzed at 24 h post treatment by qPCR with corresponding primer pairs (Table 1) using murine β-actin gene as an internal control. The reaction conditions and reagents of aforementioned qPCR assays are identical to the details mentioned in section 2.9. In order to confirm the success of transfection and analyze the downstream gene expression further, the expression level of transfected RfCytB was assessed by qPCR at 48 h post infection (p.i).

2.6. Animal rearing and tissue collection

Healthy fish (*Sebastes schlegelii*) acclimatized to laboratory conditions were obtained from one of the aquariums in the Marine Science Institute of Jeju National University, Jeju Self Governing province, Republic of Korea, and maintained in 400-L laboratory aquarium tanks filled with aerated seawater at 18 ± 1 °C. Five healthy fish with an average body weight of ~35 g were sacrificed for tissue collection. Before the sacrifice, ~1 mL of blood was collected from each fish using sterile syringes coated with 0.2% heparin sodium salt (USB, USA) and the peripheral blood cells were separated by immediate centrifugation at 3000 × *g* for 10 min at 4 °C. Other tissues, including head kidney, spleen, liver, gill, intestine, kidney, brain, muscle, skin, and heart, were excised and snap-frozen in liquid nitrogen and stored at −80 °C.

2.7. Immune challenge experiments

In order to investigate the modulatory properties of atypical *Aeromonas salmonocida* infection on RfCytB transcription, which is a known gram-negative bacterial threat in black rockfish aquaculture [28], healthy fish acclimatized to the laboratory conditions were intraperitoneally injected with 100 μL of live *A. salmonocida* (RFAS-1 strain – 1×10^9 CFU/mL), according to the pre-determined sub-lethal dose for the reared fish, in sterilized phosphate buffered saline (PBS). For the injection control group, fish were injected with 100 μL PBS. Head kidney and spleen tissues of the experimental animals were collected as described in section 2.6, by sacrificing at least five animals each at 6, 12, 24, 48, 72, and 120 h post-injection.

2.8. Total RNA extraction and cDNA synthesis

Total RNA was extracted from the pool of each excised tissue from five healthy fish, as well as from head kidney and spleen tissues from five immune-challenged or PBS-injected fish corresponding to each time point, using the RNAiso plus™ (TaKaRa, Japan) reagent, following the vendor's protocol. Tissue pooling was carried out as follows: 660 mg of brain tissues, ~50 mg of kidney tissues (~10 mg from each fish), ~125 mg of heart tissues (25 mg of each), and ~150 mg of all the other tissues (30 mg of each). Concentration of extracted RNA from different tissues was determined at 260 nm using a UV-spectrophotometer (Thermo scientific, USA) and diluted to 1 μg/μL. A 2.5-μg sample of RNA from selected tissues was used for cDNA synthesis using a cDNA synthesis kit (TaKaRa, Japan), following the manufacturer's instructions. Finally, this newly synthesized cDNA was diluted 40-fold (total 800 μL) and stored at −20 °C until further analysis.

2.9. RfCytB transcriptional analysis by quantitative real time PCR (qPCR)

The mRNA expression level of RfCytB was investigated in the tissues mentioned in section 2.6, and the temporal expression of RfCytB was examined in spleen and head kidney tissues. After the total RNA extraction, followed by cDNA synthesis, qPCR was carried out using the thermal cycler Dice™ real time System (TP800; TaKaRa, Japan) in a 10 μL reaction volume containing 3 μL of diluted cDNA from corresponding tissue, 5 μL of 2 × TaKaRa Ex Taq™, SYBR premix, 0.4 μL of each primer (RfCytB-qF and RfCytB-qR; Table 1), and 1.6 μL of dd H_2O. The qPCR was performed under the following conditions: 95 °C for 10 s, followed by 40 cycles of 95 °C for 5 s, 58 °C for 10 s, and 72 °C for 20 s, and a final cycle of 95 °C for 15 s, 60 °C for 30 s, and 95 °C for 15 s. The base line was set automatically by Dice™ Real Time System software (version 2.00). The RfCytB expression level was determined by the

Livak ($2^{-\Delta\Delta CT}$) method [29]. The same qPCR cycle profile was used for the internal control gene, black rockfish elongation factor α (RfEF1A; GenBank ID: KF430623 [30]). All data are represented as means ± standard deviation (SD) of relative mRNA expression of triplicates, and respective fold-changes in expression with respect to the RfEF1A gene were used for comparison. Moreover, the temporal fold-changes in expression with respect to RfCytB, detected for the immune-challenged groups, were normalized to the corresponding expression levels of PBS injected controls, considering the plausible effect of the medium of injection. To determine the statistical significance ($P < 0.05$) between the experimental and control groups, a two-tailed *t*-test was carried out.

3. Results and discussion

3.1. Sequence characterization and phylogenetic position

A DNA sequence (573 bp) homologous to the known cystatin B counterparts was identified from our black rockfish cDNA database and designated as *RfCytB*. The complete putative ORF of *RfCytB* was 291 bp long, which encodes for a protein of 97 amino acids with a predicted molecular mass of 11 kDa and theoretical iso-electric point of 6.3. Sequence details were deposited in NCBI-Genbank database (Genbank ID- MT385085). The protein sequence resembles the conserved cystatin family signature including a single cystatin-like domain, a cysteine protease inhibitory signature (residues ^{46}QLVSGTNYFIKVH^{58}) harboring pentapeptide QXVXG consensus sequence, which is located on hairpin loop of the protein, and two conserved N-terminal neighboring glycine (^{8}GG^{9}) residues (Fig. 1). Two G residues are known to constitute a wedge-shaped edge involving the inhibition of protease activity, which is complementary to the active site of papain-like cysteine proteases [8,31]. Moreover, a variant of typical cystatin family c-terminal proline-tryptophan (PW) motif was also identified in RfCytB, where tryptophan residue was replaced by a cysteine (C) residue. Such variations have also been reported previously with diverse cystatin B counterparts; for instance, the tryptophan residue of PW motif of human stefin B was replaced by histidine (H) residue [10].

According to our pairwise sequence alignment study, RfCytB shared a significant sequence compatibility with its teleostan cystatin B counterparts, with a high similarity (82.7%) and identity (68.4%) with olive flounder cystatin B, validating its homology with cystatin B counterparts (Table 2).

Our phylogenetic reconstruction separated different vertebrate and invertebrate cystatin counterparts into closely and independently clustered clades corresponding to four known different cystatin families, wherein, RfCytB was classified into family 1, showing a closer evolutionary relationship with its teleostan cystatin B counterparts, as expected (Fig. 2). According to the tree topology of teleostan cystatin B counterparts, Rock bream and European sea bass cystatin B were exclusively clustered in a close and independent clade, whereas, in accordance with the order, olive flounder, black rockfish, turbot, and zebrafish counterparts were clustered with an increasing phylogenetic distance from that clade. As expected, Cystatin B and A were clustered separately under family 1 cystatins, whereas, family 2, 3, and 4 counterparts were clustered closely and independent to each other. Moreover, family 1 cystatins showed a phylogenetically distant relationship with rest of the cystatin family members, originating from a separate ancestor. On the other hand, family 2, 3, and 4 members shared a common ancestral origin where family 2 and family 3 members exhibited a relatively close evolutionary relationship. Collectively, the deciphered phylogenetic relationship of RfCytB with different cystatin family similitudes clearly asserts its homology with teleostan cystatin B and its vertebrate ancestral origin.

3.2. Papain inhibitory activity of rRfCytB

Cystatins are known as potent inhibitors of papain family proteases [8], and some of the vertebrate and invertebrate cystatin B counterparts were shown to have detectable papain inhibitory activity. For instance, disk abalone [32] and manila clam [33] counterparts with invertebrate origin, and rock bream [23] and turbot [15] counterparts with vertebrate origin, have demonstrated concentration-dependent papain inhibitory activity. Thus, we intended to investigate the potential papain inhibitory activity of rRfCytB using different papain:rRfCytB ratios. According to the results, with increasing concentration of rRfCytB (with higher papain: rRfCytB ratios) inhibitory activity was found to increase, as expected (Fig. 3). The highest activity (76%) was noted with a papain:rRfCytB concentration ratio of 1:5. In contrast, in a study on manila clam cystatin B, the maximum inhibition (~80%) was noted for a papain:rRfCytB concentration ratio of 1:1. This comparison may reflect the lesser efficiency of rRfCytB in cysteine protease inhibition, compared with its invertebrate's counterparts. As expected, MBP-treated control did not show any significant papain inhibitory activity (~8%) compared with the rRfCytB-treated experiments up to a papain:rRfCytB concentration ratio of 4:1, suggesting the negligible interference of MBP in the fusion of rRfCytB. Taken together, these results reflect the putative dose-dependent cysteine protease inhibitory activity of rRfCytB.

3.3. Thermal stability of rRfCytB

We investigated the thermal stability of rRfCytB fusion protein by monitoring its papain inhibitory activity after heating the recombinant protein in a time-course manner. Intriguingly, rRfCytB demonstrated a significant thermal stability, showing a marked papain inhibitory activity (80%–90%) after heating rRfCytB for different time periods (Fig. 4). Even after 60 min of heating, the recombinant protein demonstrated ~83% relative residual inhibitory activity, although it was significantly lower ($p < 0.05$) activity than that of the un-heated control. It has been reported that cystatins do not form covalent bonds with cysteine proteases [34], and therefore, they do not interact tightly

```
                                                                  QLVSG
Black Rockfish    --MMCGGIGEVKDANEEVHKICESVKPHAEKQAGKTFDVFTAKTYKTQLVSGTNYFIKVH 58
Turbot            -MPLCGGLGESANADDDIQKICDSMKPHAEEKTGKSFAVFTAKTYKTQLVSGTNYFIKVH 59
Rock bream        MSMMCGGISAPLDADEDIQKMCDNVKPHAEEKAGKKYDVFTAKTYTTQIVSGTNYFIKIH 60
European seabass  MSMMCGGLNEPIDADDKIHKICETLKPHAEQRAGKTFEVFTAKSYSTQVVAGTNYFIKVH 60
Olive flounder    --MLCGGTSQPVDADEQIQKICDSMKPHAEAQAGKTFDVFVAKTYTTQCVPGTNYFIKVH 58
Human             --MMCGAPSATQPATAETQHIADQVRSQLEEKENKKFPVFKAVSFKSQVVAGTNYFIKVH 58
Mouse             --MMCGAPSATMPATAETQEVADQVKSQLESKENQKFDVFKAISFKRQIVAGTNLFIKVD 58
                     :**. .    *  . :.:.: ::.: * : .:.: ** * ::. * *.*** ***:.

Black Rockfish    VGGEDHVHLRVYKPLPCNG-EIQLSKMQHSKSSDDEIEYF 97
Turbot            VGEEEHLHIRVYKKLQCNGGEIELTSLQENKSHHDPIVYF 99
Rock bream        VGGDDHVHLRVYKKLPCHGGGLELSGMQHSKSLQDPIAYF 100
European seabass  VGGDDHVHLRVYEKLPCHGGDLELSAMQQSKSHQDPIEYF 100
Olive flounder    VGGDEHVHLRVYKKLPCNGETLELSKMLQDKRHHDPLEYF 98
Human             VGDEDFVHLRVFQSLPHENKPLTLSNYQTNKAKHDELTYF 98
Mouse             VGGDKCVHLRVFQPLPHENKPLTLSSYQTNKERHDELSYF 98
                  ** :. :*:**:: *  ..  : *:    .*  .* : **
```

Fig. 1. Multiple protein sequence alignment of vertebrate cystatin B counterparts including black rockfish cystatin B (RfCytB). Completely conserved and partially conserved residues were denoted by (*) and (: or.) symbols, respectively. At the N-terminal, two conserved neighboring glycine (G) residues and conserved Q, V, and G residues in consensus QxVxG pentapeptide sequence in cysteine protease inhibitory signature (indicated by double headed arrow) are shaded in gray color. The variant of typical cystatin family c-terminal proline-tryptophan (PW) motif (PC) is underlined on RfCytB protein sequence, and the putative motifs corresponding to other sequences are boxed.

Table 2
Percentage Identity and similarity values of RfCytB with different cystatin homologues.

No.	Name of the species	Protein	GenBank accession Number	Amino acids	Identity (%)	Similarity (%)
1	*Paralichthys olivaceus* (Olive flounder)	Cystatin-B	ACC86114	98	68.4	**82.7**
2	*Oplegnathus fasciatus* (Rock bream)	Cystatin-B	AFP50145	100	68	**84**
3	*Dicentrarchus labrax* (European seabass)	Cystatin-B	CBN81974	100	68	**88**
4	*Salmo salar* (Atlantic salmon)	Cystatin-B	ACI66582	99	66.7	**81.8**
5	*Scophthalmus maximus* (Turbot)	Cystatin-B	ADM61584	99	64.6	**84.8**
6	*Danio rerio* (Zebrafish)	Cystatin-B	NP001096599	100	64	**81**
7	*Gallus gallus* (Chicken)	Cystatin-B	NP001185577	98	51	**72.4**
8	*Homo sapiens* (Human)	Cystatin-B	NP000091	98	46.9	**65.3**
9	*Rattus norvegicus* (Rat)	Cystatin-B	NP036970	98	45.9	**63.3**
10	*Mus musculus* (Mouse)	Cystatin B	NP031819	98	44.9	**62.2**
11	*Homo sapiens* (Human)	Cystatin-A	NP005204	98	41.8	**65.3**
12	*Mus musculus* (Mouse)	Cystatin-A	NP001028411	97	40.2	**66**
13	*Rattus norvegicus* (Rat)	Cystatin A	NP001099346	97	40.2	**64.9**
14	Bos taurus (Bovine)	Cystatin A	NP001161296	98	39.8	**65.3**
15	*Mus musculus* (Mouse)	Cystatin C	AAA63298	140	19.7	**32.1**
16	*Onchocerca volvulus*	CPI	P22085	162	16.2	**30.9**
17	*Rattus norvegicus* (Rat)	Cystatin C	NP036969	140	16.2	**32.1**
18	*Bos taurus* (Bovine)	Cystatin C	NP776454	148	15	**32.4**
19	*Homo sapiens* (Human)	Cystatin C	NP_000090	146	14.9	**31.5**
20	*Saimiri sciureus* (Monkey)	Cystatin C	O19093	146	14.8	**28.1**
21	*Acanthocheilonema viteae* (Rodent filaria worm)	Cystatin	AAA87228	157	14.6	**31.2**
22	*Brugia malayi* (Filaria nemotode worm)	CPI-2	AAD51086	161	14.3	**29.8**
23	*Homo sapiens* (Human)	Cystatin D	CAA49838	142	13.9	**27.5**
24	*Mus musculus* (Mouse)	Kininogen	NP075614	432	9	**15.7**
25	*Homo sapiens* (Human)	Kininogen	NP000884	427	8.7	**12.9**
26	*Bos taurus* (Bovine)	Kininogen	NP001106748	619	6.8	**10.5**
27	*Rattus norvegicus* (Rat)	Kininogen	NP036873	639	6.3	**9.1**

with the proteases. On the other hand, they can cover the active site cleft to obstruct the access of the relevant substrate to the active site of the proteases. Therefore, structural damage of cystatins, elicited by environmental factors such as high temperatures, may not severely alter its cysteine protease inhibitory activity, in accordance with the observations regarding rRfCytB. However, showing a contrasting outcomes to what we have observed, recombinantly expressed cystatin counterpart of Chinese sturgeon was found to lose its papain inhibitory activity with heating even at 70 °C in time course experiment, initially with high rate and later low rate of papain inhibitory activity reduction with the time, up to 40% of initial activity (after 60 min of heating) with unheated control [35].

3.4. Transfection of rRfCytB

The transfection study, conducted to observe the modulation of marker genes of an inflammatory condition in murine macrophages upon cystatin B over-expression, displayed positive results from the subsequent qPCR analysis. The transcription level of *RfCytB* was much higher than that of the control cells, indicating that the RfCytB was overproduced in transfectants, thereby confirming the overexpression of *RfCytB* in murine macrophages (Fig. 5A). Further analysis of immune-related genes associated with inflammatory conditions caused by Cystatin B overexpression revealed an increased expression of iNOS and TNF-α (Fig. 5B). Cystatin B and two other cystatins are known to induce the release of nitric oxide (NO) from activated macrophages [36,37]. Previous studies have shown that the cystatins induce NO release via synthesis of TNF-α and IL-10 [10]. These results demonstrate the relationships underlying the regulation of CytB, TNF-α, and iNOS. These findings further ascertain the importance of cystatin B in teleost innate immune system related to bacterial infection.

3.5. Tissue specific mRNA expression

According to the results of our qPCR assay, ubiquitous expression of *RfCytB* was detected in the tissues examined, albeit at different levels (Fig. 6). The expression was particularly pronounced in gill and spleen tissues, whereas the lowest expression levels were observed in muscle and liver tissues. The gills are frequently in contact with outer environment, which makes them more vulnerable towards pathogen infections. Cystatins, including cystatin B, are involved in disease pathology in addition to normal proteolysis processes, wherein they are known to modulate the immune responses against invading pathogens [38]. Therefore, a pronounced level of RfCytB expression is expected in gill tissues, which may involve the inhibition of crucial cysteine proteases in pathogens such as bacteria, viruses, or parasites, in order to suppress their proliferation and survival in host cells. Spleen is the largest lymphoid organ in teleosts, harboring essential cellular components of innate immunity, including aggregates of macrophages (melanomacrophages) [39,40]. On the other hand, teleostan cystatin B have been shown to have an antimicrobial effect on teleostan macrophages [15] and up-regulate the nitric oxide (NO) release from IFN-γ-activated murine macrophages [13,36]. Thus, the high expression of RfCytBs in the spleen could modulate the aforementioned immune functions of the melanomacrophages.

Congruent with the tissue-specific expression of RfCytB, ubiquitous expression of olive flounder cystatin B was detected in the examined tissues, with a prominent expression detected in gill tissues [41]. Moreover, the expression of manila clam cystatin B was reported in all the tested tissues, with pronounced mRNA expression levels observed in hemocytes as well as gill tissues [33]. However, in contrast to RfCytB tissue expression, the turbot cystatin B mRNA was expressed abundantly in muscle tissues and weakly in spleen, blood, gill, and kidney tissues. On the other hand, within the detected universal tissue-specific transcriptional profile of rock bream cystatin B, liver tissues showed an eminent mRNA expression, followed by spleen, gill, brain, and intestine [23]. However, muscle tissues showed the lowest level of cystatin B mRNA expression in rock bream, consistent with our observation on RfCytB tissue-specific transcription.

3.6. Transcriptional response to experimental pathogen infection

In order to prefigure the potential importance of RfCytB on host immune responses, we sought to decipher its temporal transcriptional responses to experimental infection, using a known pathogen of black rockfish, *A. salmonocida*. Our qPCR assays revealed a significant

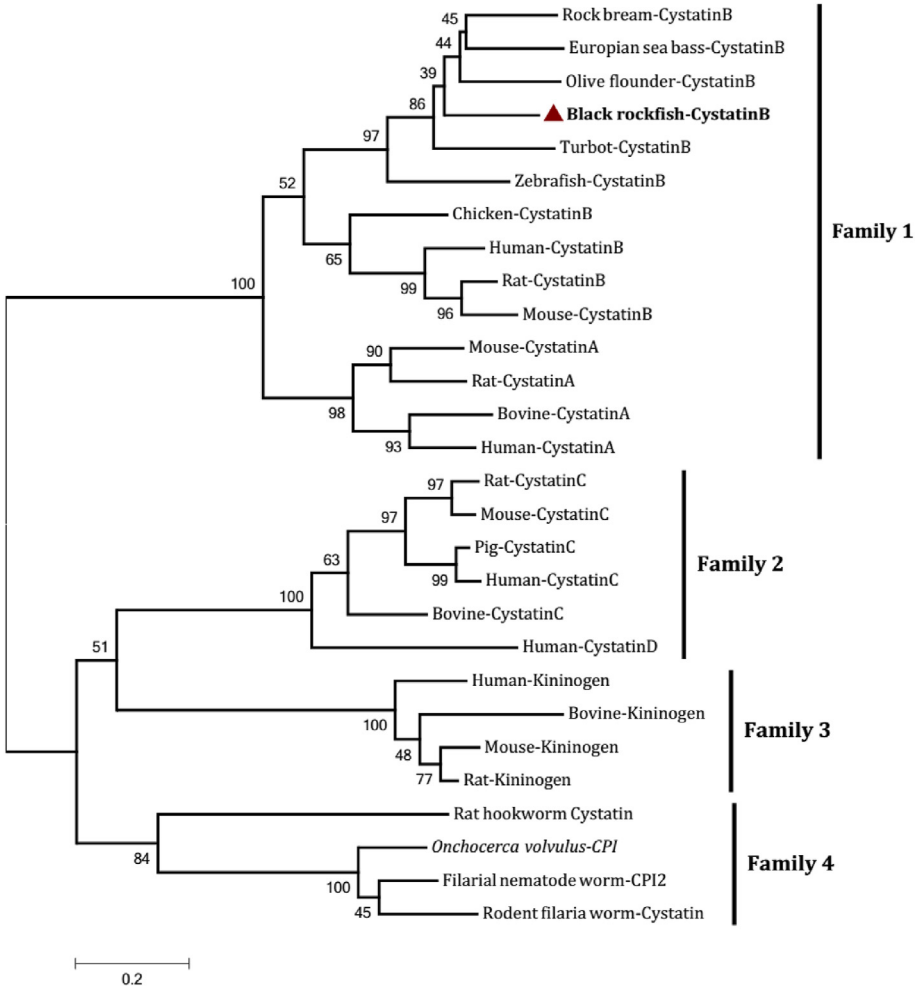

Fig. 2. Phylogenetic position of RfCytB, analyzed by MEGA version 6.0 software based on ClustalW2 multiple sequence alignment of different vertebrates and invertebrate counterparts under the neighbor-joining platform. Corresponding bootstrap values are denoted at the tree branches and NCBI-GenBank accession numbers of the used cystatin homologues are mentioned in Table 2.

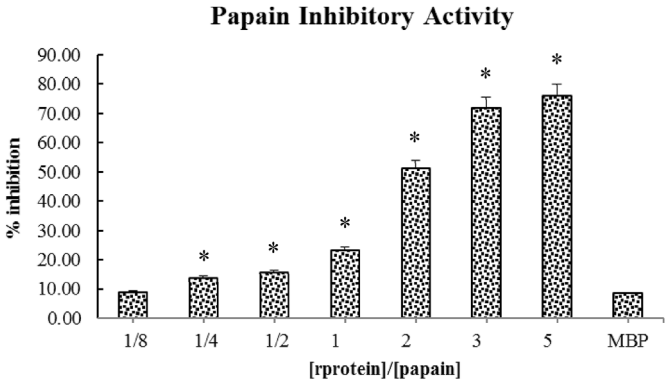

Fig. 3. *In vitro* papain inhibitory activity at different concentrations of rRfCytB. Azo-casein was used as the substrate for papain enzyme, and MBP was used as a control. Error bars represent SDs ($n = 3$) and asterisk represents statistically different ($P < 0.05$) inhibition levels compared with the% inhibition of MBP-treated control.

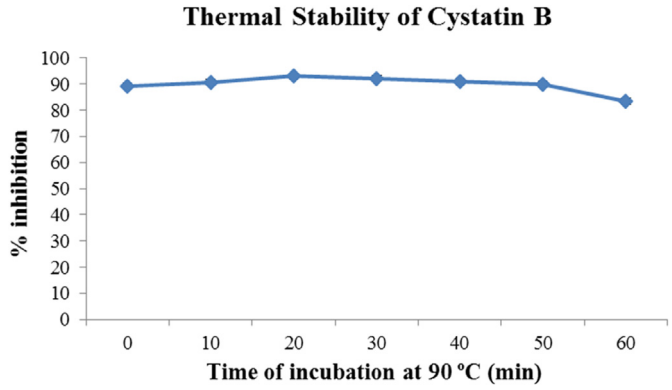

Fig. 4. Thermal stability of RfCytB with time, monitored using the papain inhibitory activity after heating the recombinant protein in a time-course manner.

modulation of *RfCytB* in spleen as well as head kidney tissues in response to the live bacterial infection. Upon the infection, the mRNA expression of RfCytB at 12 h p.i. was up-regulated in spleen tissues by ~3.4 fold compared with its basal level (0 h p.i.)), with a significant ($P < 0.05$) down-regulation observed at 3 h p.i (Fig. 7A). Interestingly, the head kidney showed a noticeable transcriptional modulation, exclusively with inductive transcriptional responses against the infection at early, middle, as well as late phase p.i. (6 h, 12 h, and 48 h p.i.), wherein a more pronounced fold-increase (~45 fold) was observed at 12 h p.i., compared with the basal level (Fig. 7B). However, in comparison with the transcriptional responses of head kidney and spleen, a more marked modulation of RfCytB could be observed in head kidney than in spleen, compared with its basal level expression. Teleostan head

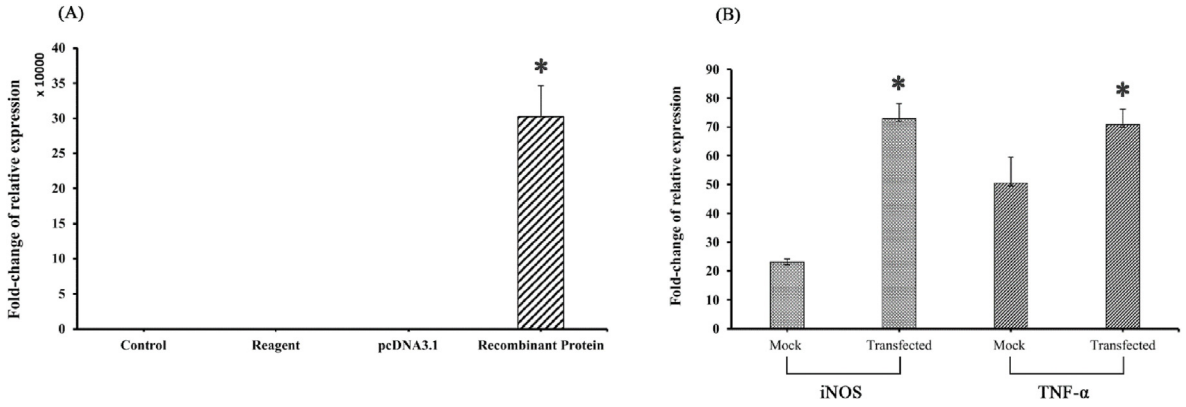

Fig. 5. Gene expression analysis of transfection study by qPCR. The empty pcDNA3.1 vector and pcDNA3.1-RfCytB were transfected into murine macrophage cells. After 24 h of transfection, the cells were treated with LPS and then harvested after 24 h. RNA was isolated, cDNA was prepared, and the gene expression was analyzed by qPCR. The expression was normalized to that of β-actin in mock controls. **(A)** rRfCytB gene expression in control (without any treatment), transfection-reagent-treated control, mock control, and the transfected cells. The values were normalized to that of the control. **(B)** Expression patterns of iNOS and TNF-α genes post transfection in pcDNA3.1-RfCytB-transfected cells and corresponding mock controls. The significant differences in expression levels were compared with the expression in the mock controls. Error bars represent SDs (n = 3), and the asterisks indicate the significant differences ($P < 0.05$) obtained from *t*-test.

kidneys and spleens are both enriched with macrophages aggregating into melanomacrophage centers [40]. As cystatins are known to be involved in antimicrobial defense in teleostan macrophages, it can be assumed that, upon pathogen infection, overexpression of cystatins is expected to be involved in host immune responses that elicit pathogen clearance. Taken together, the detected transcriptional responses of RfCytB against our bacterial infection suggest its putative importance in the host antibacterial defense.

Congruent with the results of our experimental challenge experiment, rock bream cystatin was reported to have elevated mRNA expression level post *in-vivo Edwardisella tarda* treatment in head kidney and spleen tissues, with a marked fold-increase observed in head kidney tissues [32]. Moreover, the same stimulus could trigger inductive transcriptional responses of turbot cystatin B gene in kidney, spleen, brain, and liver tissues within 24 h p.i [15]. In contrast, as reported previously, olive flounder cystatin B was not significantly induced in kidney and gill tissues upon treatment with a well-known bacterial endotoxin, lipopolysaccharide, but a slight induction was observed in muscle and spleen tissues at 24 h post treatment [41].

4. Conclusion

In conclusion, the current study reports the identification and functional characterization of Cystatin B from Korean black rockfish. Cystatin B was evolutionarily conserved from fish to mammals. It was ubiquitously expressed in different tissues and the expression fluctuated upon bacterial simulation. Moreover, over-expression of RfCytB could trigger the up-regulation of pro-inflammatory genes in murine

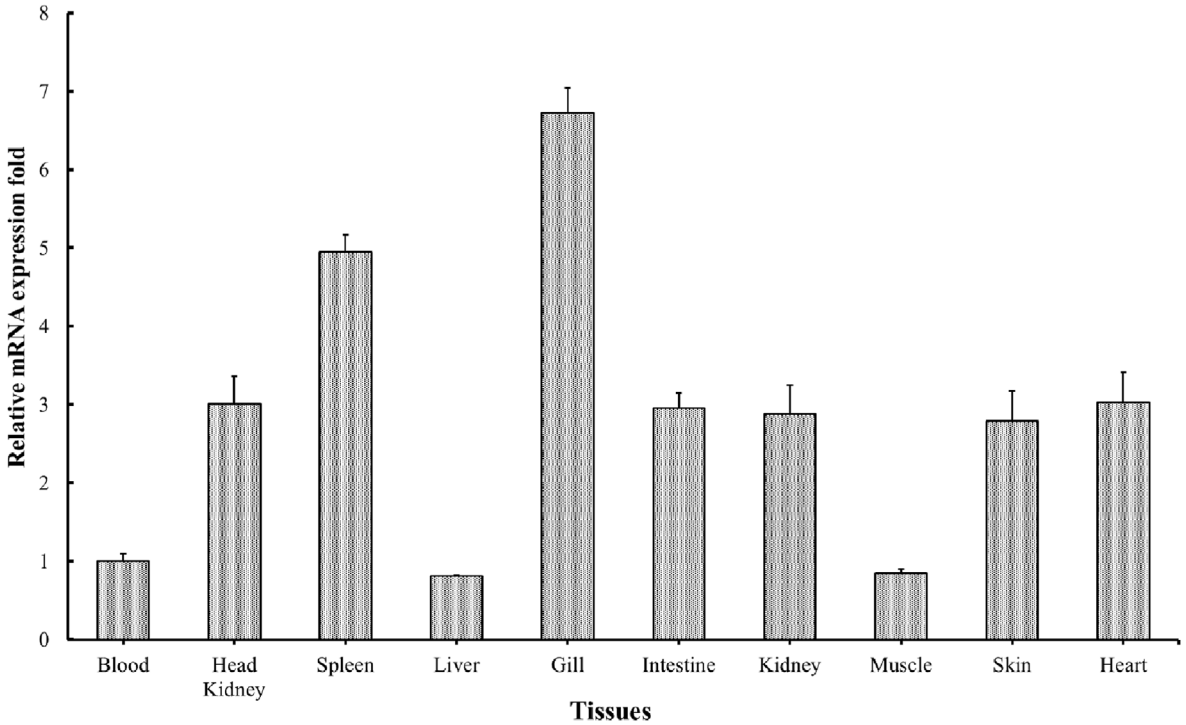

Fig. 6. Spatial expression of RfCytB was determined by quantitative real-time PCR in various tissues of unchallenged black rockfish. The Livak method was used to determine the relative mRNA expression, and the elongation factor-1α of black rockfish was used as a reference gene. Vertical bars represent the SD.

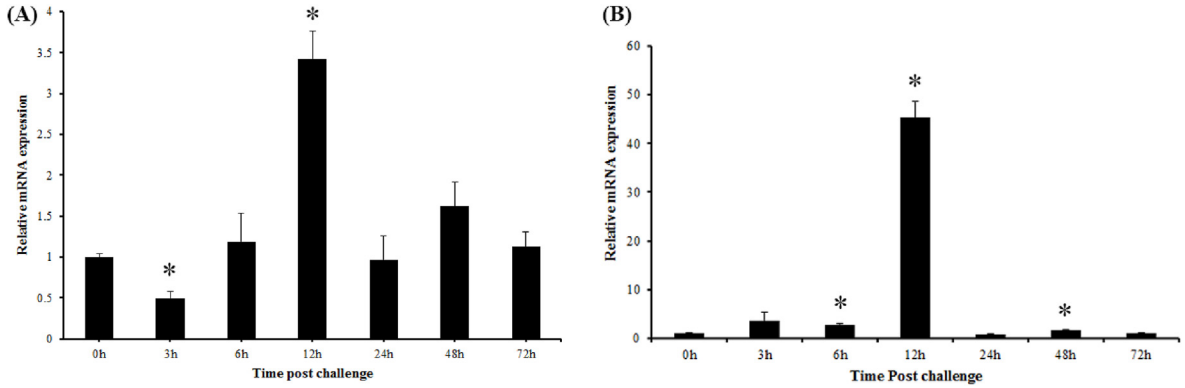

Fig. 7. The temporal mRNA expression of RfCytB in spleen **(A)** and Head kidney **(B)** tissues of rockfish after *A. salmonocida* injection, as detected by SYBR green qPCR. The relative expression was calculated using the $2^{-\Delta\Delta CT}$ method, using black rockfish elongation factor α as the internal reference gene. All the values were normalized to corresponding PBS-injected controls at each time point. The relative fold-change in expression at 0 h post-injection was used as the baseline. Error bars represent ± SD (n = 3), and the asterisks indicate the significant differences ($P < 0.05$).

macrophages. Collectively, these findings on rockfish Cystatin B provide insights into the role of Cystatin B in fish lineages.

CRediT authorship contribution statement

P.D.S.U. Wickramasinghe: Conceptualization, Data curation, Formal analysis, Investigation, Methodology, Writing - original draft. **Hyukjae Kwon:** Formal analysis, Investigation, Methodology, Writing - original draft. **Don Anushka Sandaruwan Elvitigala:** Conceptualization, Formal analysis, Writing - review & editing. **Qiang Wan:** Writing - review & editing. **Jehee Lee:** Conceptualization, Funding acquisition, Project administration, Writing - review & editing.

References

[1] N.D. Rawlings, A.J. Barrett, MEROPS: the peptidase database, Nucleic Acids Res. 27 (1999) 325–331, https://doi.org/10.1093/nar/27.1.325.
[2] G.N. Rudenskaya, D.V. Pupov, Cysteine proteinases of microorganisms and viruses, Biochemistry 73 (2008) 1–13, https://doi.org/10.1134/S000629790801001X.
[3] H.A. Chapman, R.J. Riese, G.-P. Shi, Emerging roles for cysteine proteases in human biology, Annu. Rev. Physiol. 59 (1997) 63–88, https://doi.org/10.1146/annurev.physiol.59.1.63.
[4] L.K. Ward-Kavanagh, W.W. Lin, J.R. Šedý, C.F. Ware, The TNF receptor superfamily in Co-stimulating and Co-inhibitory responses, Immunity 44 (2016) 1005–1019, https://doi.org/10.1016/j.immuni.2016.04.019.
[5] M.E. McGrath, The lysosomal cysteine proteases, Annu. Rev. Biophys. Biomol. Struct. 28 (1999) 181–204, https://doi.org/10.1146/annurev.biophys.28.1.181.
[6] E. Amri, F. Mamboya, Papain, a plant enzyme of biological importance: a review, Am. J. Biochem. Biotechnol. 8 (2012) 99–104, https://doi.org/10.3844/ajbbsp.2012.99.104.
[7] R.T. Shenoy, S. Thangamani, A. Velazquez-Campoy, B. Ho, J.L. Ding, J. Sivaraman, Structural basis for dual-inhibition mechanism of a non-classical kazal-type serine protease inhibitor from horseshoe crab in complex with subtilisin, PloS One 6 (2011), https://doi.org/10.1371/journal.pone.0018838.
[8] M. Abrahamson, Cystatins - protein inhibitors of papain-like cysteine proteinases, Cienc Cult. (Sao Paulo) 45 (1993) 299–299.
[9] W. Bode, R. Huber, Structural basis of the endoproteinase-protein inhibitor interaction, Biochim. Biophys. Acta Protein Struct. Mol. Enzymol. 1477 (2000) 241–252, https://doi.org/10.1016/S0167-4838(99)00276-9.
[10] Josiah Ochieng, Gautam Chaudhuri, J. Cystatin Superfamily, Health Care Poor Underserved 21 (2010) 51–70, https://doi.org/10.1353/hpu.0.0257.
[11] G.A. Cornwall, N. Hsia, At the Cutting Edge A new subgroup of the family 2 cystatins, Mol. Cell. Endocrinol. 200 (2003) 1–8.
[12] W.M. Brown, K.M. Dziegielewska, Friends and relations of the cystatin superfamily–new members and their evolution, Protein Sci. 6 (1997) 5–12, https://doi.org/10.1002/pro.5560060102.
[13] L. Verdot, G. Lalmanach, V. Vercruysse, S. Hartmann, R. Lucius, J. Hoebeke, F. Gauthier, B. Vray, Cystatins up-regulate nitric oxide release from interferon-γ-activated mouse peritoneal macrophages, J. Biol. Chem. 271 (1996) 28077–28081, https://doi.org/10.1074/jbc.271.45.28077.
[14] L. Verdot, G. Lalmanach, V. Vercruysse, J. Hoebeke, F. Gauthier, B. Vray, Chicken cystatin stimulates nitric oxide release from interferon-γ- activated mouse peritoneal macrophages via cytokine synthesis, Eur. J. Biochem. 266 (1999) 1111–1117, https://doi.org/10.1046/j.1432-1327.1999.00964.x.
[15] P.P. Xiao, Y.H. Hu, L. Sun, Scophthalmus maximus cystatin B enhances head kidney macrophage-mediated bacterial killing, Dev. Comp. Immunol. 34 (2010) 1237–1241, https://doi.org/10.1016/j.dci.2010.07.008.
[16] R. Di Giaimo, New insights into the molecular basis of progressive myoclonus epilepsy: a multiprotein complex with cystatin B, Hum. Mol. Genet. 11 (2002) 2941–2950, https://doi.org/10.1093/hmg/11.23.2941.
[17] M. Takahashi, T. Tezuka, N. Katunuma, Inhibition of growth and cysteine proteinase activity of Staphylococcus aureus V8 by phosphorylated cystatin α in skin cornified envelope, FEBS Lett. 355 (1994) 275–278, https://doi.org/10.1016/0014-5793(94)01196-6.
[18] X.-P. Zhong, D. Wang, Y.-B. Zhang, J.-F. Gui, Identification and characterization of hypoxia-induced genes in Carassius auratus blastulae embryonic cells using suppression subtractive hybridization, Comp. Biochem. Physiol. B Biochem. Mol. Biol. 152 (2009) 161–170, https://doi.org/10.1016/j.cbpb.2008.10.013.
[19] B. Rajan, J.M.O. Fernandes, C.M.A. Caipang, V. Kiron, J.H.W.M. Rombout, M.F. Brinchmann, Proteome reference map of the skin mucus of Atlantic cod (Gadus morhua) revealing immune competent molecules, Fish Shellfish Immunol. 31 (2011) 224–231, https://doi.org/10.1016/j.fsi.2011.05.006.
[20] L. Wang, P. Liu, S. Huang, B. Ye, E. Chua, Z.Y. Wan, G.H. Yue, Genome-wide association study identifies loci associated with resistance to viral nervous necrosis disease in asian seabass, Mar. Biotechnol. 19 (2017) 255–265, https://doi.org/10.1007/s10126-017-9747-7.
[21] D.M. Patel, M.F. Brinchmann, Skin mucus proteins of lumpsucker (Cyclopterus lumpus), Biochem. Biophys. Reports. 9 (2017) 217–225, https://doi.org/10.1016/j.bbrep.2016.12.016.
[22] J.W. Wynne, M.G. O'Sullivan, M.T. Cook, G. Stone, B.F. Nowak, D.R. Lovell, N.G. Elliott, Transcriptome analyses of amoebic gill disease-affected atlantic salmon (Salmo salar) tissues reveal localized host gene suppression, Mar. Biotechnol. 10 (2008) 388–403, https://doi.org/10.1007/s10126-007-9075-4.
[23] H.K.A. Premachandra, I. Whang, Y.D. Lee, S. Lee, M. De Zoysa, M.J. Oh, S.J. Jung, B.S. Lim, J.K. Noh, H.C. Park, J. Lee, Cystatin B homolog from rock bream Oplegnathus fasciatus: genomic characterization, transcriptional profiling and protease-inhibitory activity of recombinant protein, Comp. Biochem. Physiol. B Biochem. Mol. Biol. 163 (2012) 138–146, https://doi.org/10.1016/j.cbpb.2012.05.012.
[24] D.A.S. Elvitigala, T.T. Priyathilaka, I. Whang, B.H. Nam, J. Lee, A teleostan homolog of catalase from black rockfish (Sebastes schlegelii): insights into functional roles in host antioxidant defense and expressional responses to septic conditions, Fish Shellfish Immunol. 44 (2015) 321–331, https://doi.org/10.1016/j.fsi.2015.02.020.
[25] D.G. H, T.J. G, Julie D. Thompson, CLUSTALW: improving the sensitivity of progressive multiple sequence alignment through sequence weighting, position-specific gap penalties and weight matrix choice, Nucleic Acids Res. 22 (1994) 4673–4680. Thompson, Julie D.; Higgins, Desmond G.; Gibson, Toby J.
[26] J.J. Campanella, L. Bitincka, J. Smalley, MatGAT: an application that generates similarity/identity matrices using protein or DNA sequences, BMC Bioinf. 4 (2003) 1–4, https://doi.org/10.1186/1471-2105-4-29.
[27] K. Tamura, G. Stecher, D. Peterson, A. Filipski, S. Kumar, MEGA6: molecular evolutionary genetics analysis version 6.0, Mol. Biol. Evol. 30 (2013) 2725–2729, https://doi.org/10.1093/molbev/mst197.
[28] I.É.Â.Ä.Í. Šw, R. August, Atypical Aeromonas Salmonicida Black Infection Rockfish in Cultured Schlegel ' S Koichi Izumikawa * 1 and Noriyuki Ueki * 1 * 1Okayama Prefectural Fisheries Experiment Station, Ushimado , Okayama 701-43 , Japan, (n. d.) 0–1.
[29] K.J. Livak, T.D. Schmittgen, Analysis of relative gene expression data using real-time quantitative PCR and, Methods 25 (2001) 402–408, https://doi.org/10.1006/meth.2001.1262.
[30] M. Liman, W. Wenji, L. Conghui, Y. Haiyang, W. Zhigang, W. Xubo, Q. Jie, Z. Quanqi, Selection of reference genes for reverse transcription quantitative real-time PCR normalization in black rockfish (Sebastes schlegeli), Mar. Genomics. 11 (2013) 67–73, https://doi.org/10.1016/j.margen.2013.08.002.
[31] W. Bode, R. Engh, D. Musil, U. Thiele, R. Huber, A. Karshikov, J. Brzin, J. Kos, V. Turk, The 2.0 A X-ray crystal structure of chicken egg white cystatin and its possible mode of interaction with cysteine proteinases, EMBO J. 7 (1988)

2593–2599 http://www.ncbi.nlm.nih.gov/pubmed/3191914.
[32] H.K.A. Premachandra, Q. Wan, D.A.S. Elvitigala, M. De Zoysa, C.Y. Choi, I. Whang, J. Lee, Genomic characterization and expression profiles upon bacterial infection of a novel cystatin B homologue from disk abalone (Haliotis discus discus), Dev. Comp. Immunol. 38 (2012) 495–504, https://doi.org/10.1016/j.dci.2012.06.010.
[33] H.K.A. Premachandra, D.A.S. Elvitigala, I. Whang, E. Kim, M. De Zoysa, B.-S. Lim, S.-Y. Yeo, S. Kim, M.-A. Park, H.-C. Park, J. Lee, Expression profile of cystatin B ortholog from Manila clam (Ruditapes philippinarum) in host pathology with respect to its structural and functional properties, Fish Shellfish Immunol. 34 (2013) 1505–1513, https://doi.org/10.1016/j.fsi.2013.03.349.
[34] H. Kwon, H. Yang, S. Lee, J. Nilojan, S.D.N.K. Bathige, B.H. Nam, Q. Wan, J. Lee, Characterization of a Kazal-type serine protease inhibitor from black rockfish Sebastes schlegelii and its possible role in hepatic immune response, Fish Shellfish Immunol. 74 (2018) 485–490, https://doi.org/10.1016/j.fsi.2017.12.068.
[35] J. Bai, D. Ma, H. Lao, Q. Jian, X. Ye, J. Luo, X. Xong, Y. Li, X. Liang, Molecular cloning, sequencing, expression of Chinese sturgeon cystatin in yeast Pichia pastoris and its proteinase inhibitory activity, J. Biotechnol. 125 (2006) 231–241, https://doi.org/10.1016/j.jbiotec.2006.02.023.
[36] S. Hartmann, A. Schönemeyer, B. Sonnenburg, B. Vray, R. Lucius, Cystatins of filarial nematodes up-regulate the nitric oxide production of interferon-gamma-activated murine macrophages, Parasite Immunol. 24 (2002) 253–262 http://www.ncbi.nlm.nih.gov/pubmed/12060319.
[37] M.A. Marietta, Minireview nitric oxide synthase structure and mechanism, J. Biol. Chem. 268 (1993) 12231–12234.
[38] T. Zavasnik-bergant, [Frontiers in bioscience 4625-4637, may 1, 2008] cystatin protease inhibitors and immune functions Tina zavasnik-bergant, Bioscience (2008) 1–13.
[39] A. Zapata, B. Diez, T. Cejalvo, C. Gutiérrez-de Frías, A. Cortés, Ontogeny of the immune system of fish, Fish Shellfish Immunol. 20 (2006) 126–136, https://doi.org/10.1016/j.fsi.2004.09.005.
[40] C. Uribe, H. Folch, R. Enriquez, G. Moran, Innate and adaptive immunity in teleost fish: a review, Vet. Med. 56 (2011) 486–503 http://vri.cz/docs/vetmed/56-10-486.pdf.
[41] S.J. Ahn, H.J. Bak, J.H. Park, S.A. Kim, N.Y. Kim, J.Y. Lee, J.H. Sung, S.J. Jeon, J.K. Chung, H.H. Lee, Olive flounder (Paralichthys olivaceus) cystatin B: cloning, tissue distribution, expression and inhibitory profile of piscine cystatin B, Comp. Biochem. Physiol. B Biochem. Mol. Biol. 165 (2013) 211–218, https://doi.org/10.1016/j.cbpb.2013.04.007.